

Liver Histopathological Changes Related to Intraperitoneal Administration of Salicylic Acid/Fe₃O₄ Nanoparticles to C57BL/6 Mice

BOGDAN MÎNDRILĂ¹, ION ROGOVEANU², SANDRA-ALICE BUTEICĂ³,
LILIANA CERCELARU⁴, DAN-EDUARD MIHAIESCU⁵,
MARINA-DANIELA MĂNESCU¹, ION MÎNDRILĂ⁴, IONICA PIRICI⁴

¹Doctoral School, University of Medicine and Pharmacy of Craiova, Romania

²Department of Gastroenterology, Faculty of Medicine
University of Medicine and Pharmacy of Craiova, Romania

³Faculty of Pharmacy, University of Medicine and Pharmacy of Craiova, Romania

⁴Department of Morphology, Faculty of Medicine,
University of Medicine and Pharmacy of Craiova, Romania

⁵Faculty of Applied Chemistry and Materials Science, University Politehnica of Bucharest, Romania

ABSTRACT: With a simple synthesis and easy engineering of physicochemical properties, iron oxide nanoparticles (IONPs) have become widely used in multiple biomedical applications. The study of IONPs toxicity has become an important issue, especially as the results reported so far are contradictory and range from lack of toxicity to cellular toxicity. The aim of this study was to evaluate the histopathological changes induced in mouse liver by long-term intraperitoneal injection of low doses of IONPs functionalized with salicylic acid (SalIONPs). The study was performed on C57BL/6 mice that received by intraperitoneal injection (IP), every two days, 0.6ml of SalIONPs aqueous suspension (35mg/kg body weight SalIONPs that contained 20mg/kg body weight of Fe₃O₄) for 28 days. The results of this study showed that the cumulative dose of 105mg/kg body weight SalIONPs (62mg/kg body weight of Fe₃O₄) induced histopathological changes in the subcapsular region of the mouse liver, possible by the release of salicylic acid into the peritoneal cavity. The cumulative dose of 244mg/kg body weight SalIONPs (145mg/kg body weight of Fe₃O₄) induced liver centrilobular necrosis, which requires the use of lower doses in biological applications. However, this may prove to be beneficial in the case of targeted accumulation of SalIONPs.

KEYWORDS: Iron oxide nanoparticles, salicylic acid, toxicity, rat liver, hidropic degeneration.

Introduction

IONPs have been extensively studied in recent decades because they can be synthesized by affordable methods [1] and their physicochemical properties can be specifically engineered for multiple biomedical applications [2], including hyperthermia [3], magnetic resonance imaging [4], cancer therapy [5,6], iron replacement therapy [7], regenerative medicine and tissue engineering [8], among others.

In order to improve their stability, biocompatibility and pharmacokinetics, the nanoparticles were functionalized by coating with natural and synthetic polymers [9-11], surfactants [12], organic compounds [13] or bioactive molecules [14].

As the number of nanoproducts with clinical applicability increases, the biosafety of IONPs begins to become a subject of public interest [15].

Numerous in vitro or in vivo IONPs toxicity studies have been performed to date, some with conflicting results. The shape, size, and type of

core of the IONPs but also the form of administration and the cell line tested are factors that influence the biocompatibility and toxicity of IONPs and may explain the different results of these studies [2,16].

The liver and spleen are the primary organs in which nanoparticles accumulate, regardless of the administration route [17].

IONPs accumulate in a proportion of 80-90% in the liver, 5-8% in the spleen and 1-2% in the bone marrow, so investigating the hepatotoxicity profile of the IONPs becomes a critical step before initiating clinical trials [18].

IONPs administration at 75 mg/kg/day for three consecutive days did not induce hepatic histopathological effects or level changes of liver enzymes in rats [19].

However, some in vitro or in vivo studies have reported cytotoxic effects of IONPs by ROS generation, iron release, genetic effects, induction of autophagy or apoptosis [17,20-23], and their toxicity appears to be dependent on concentration, exposure time and surface coating [15].

IONPs incorporation in liver macrophages can be increased with coating materials that induce a high positive or negative surface charge [24].

Salicylic acid increases membrane permeability [25] and provide a negative charge [26] that increases the cell uptake [27].

Therefore, salicylic acid coating may be considered the key factor responsible for the preferential retention of salicylic acid/IONPs functionalized nanoparticles (SaIONPs) in hepatocyte and Kupffer cells [28].

On the other hand, increased salicylate levels can lead to liver damage such as microvesicular steatosis [29], and the additive effect can increase the IONPs hepatic toxicity.

Based on these considerations, the aim of the present study is to investigate in vivo the dynamics of histopathological changes induced in liver by long-term IP administration of low doses of SaIONPs. The study was performed on C57BL/6 mice that received every two days 0.6ml of SaIONPs aqueous suspension administered IP for 28 days.

Material and Methods

Functionalized IONPs Aqueous Dispersion

For this study we used the SaIONPs synthesized by Massart method modified, as presented by some of us [28].

Dispersion in ultrapure water of SaIONPs had an average hydrodynamic diameter of 73nm, polydispersity index of 0.14, zeta potential of +50.5mV, Fe₃O₄ concentration of 0.67mg/ml and estimated salicylic acid content of 0.46=mg/ml.

Animals

8-week-old male C57BL/6 mice (n=12) with an average weight of 19.5±2.1g obtained from the Animal Facility of the University of Medicine and Pharmacy of Craiova were used.

Throughout the experiment the mice were kept in stainless steel cages, with free access to water and standard laboratory food, in the following environmental conditions: temperature of 21°C, humidity of 55% and light/night cycle of 12 hours.

The approvals for the animal study were obtained from the Committee of Ethics and Scientific Deontology according to the procedures of the University of Medicine and Pharmacy of Craiova.

Mice were randomly divided into two groups: the control group (n=4), who received

0.6ml of ultrapure water every two days intraperitoneally; the treated group (n=8), which received IP 0.6ml of aqueous dispersion of SaIONPs (35mg/kg body weight SaIONPs that contained 20mg/kg body weight of Fe₃O₄) every two days.

Two mice from the treated group and one mouse from the control group were sacrificed and autopsied on days 7, 14, 21 and 28 of the experiment, and the liver was harvested for histopathological study.

Histopathology

Liver samples collected from autopsied mice were fixed for 48 hours in 10% buffered formalin, processed for paraffin embedding, cut into 7µm thick sections using a Leica RM2255 rotary microtome, and collected on poly-L-lysine coated slides.

Light microscopy analysis of liver lesions was performed on HE and Masson trichromic Goldner stained sections. Ferric ion labeling by specific Perls Prussian blue staining was used to identify SaIONPs deposits in the liver parenchyma. The relative area of SaIONPs deposits (RAD) on Perl Prussian blue-stained sections was used to compare the SaIONPs load of the studied livers: RAD=SaIONPs deposits area *100/measured area.

For this, 20 fields taken with the x20 objective from each studied liver were analyzed with the Image-Pro Plus software. The results were shown as mean±SD. The data were compared with the Mann-Whitney U test, with a significance level of 0.05 using SPSS (version 16) software.

Results

SaIONPs liver passage

IP administered SaIONPs were identified in the portal vein as aggregates visible in light microscopy, or in the cytoplasm of circulating macrophages (Figure 1a).

Some of them can cross the wall of the large veins directly to reach the adjacent liver parenchyma. SaIONPs aggregates that passed through the sinusoids were retained by Kupffer cells or hepatocytes (Figure 1b-e).

In sinusoids, SaIONPs-loaded circulating macrophages join Kupffer cells. We used the term liver macrophages for both cell phenotypes because in the hepatic sinusoids they did not show distinctive features in Perls staining. Some of them may pass into the central venules, where they regain the morphological features of the circulating macrophages (Figure 1d).

Others have been identified crossing the liver capsule to form large clusters of SaIONPs-

loaded macrophages on its outer surface (Figure 1b).

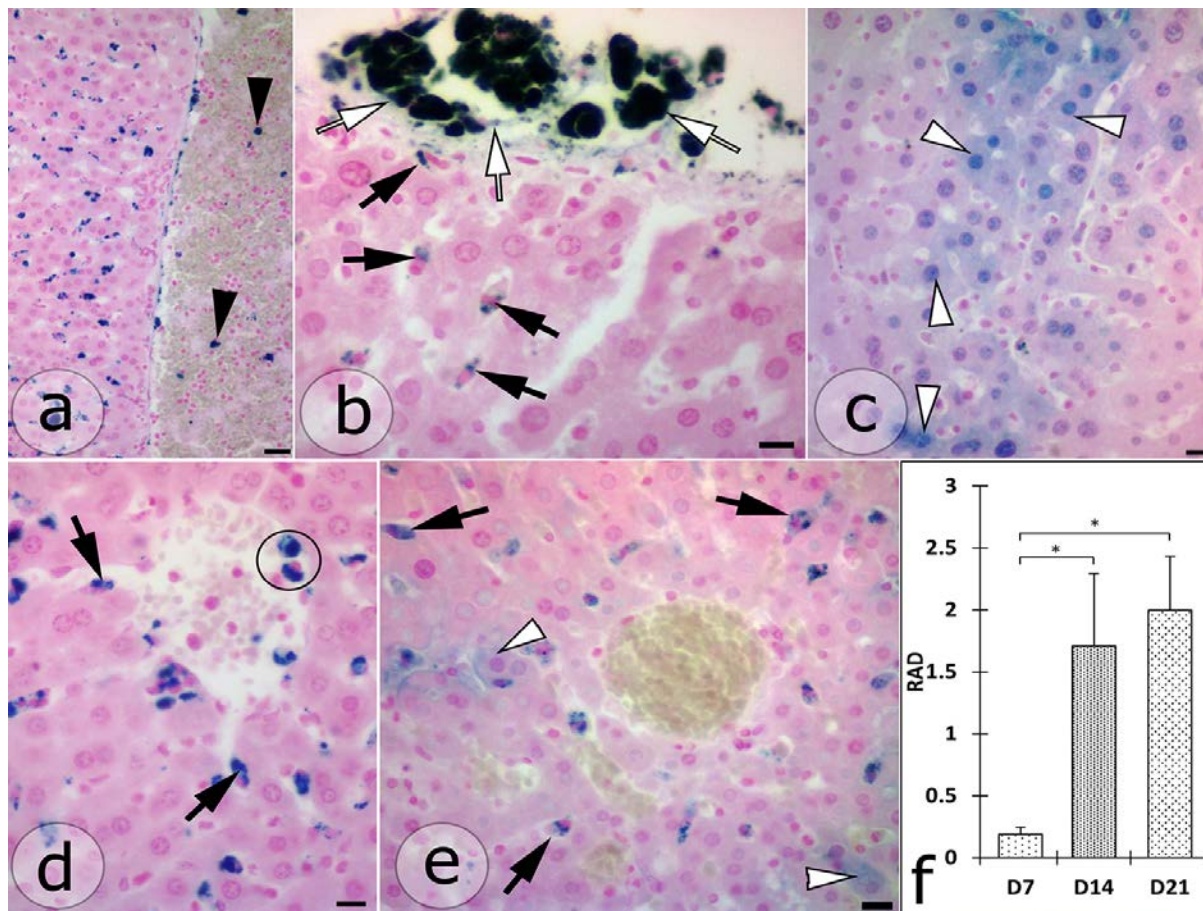


Figure 1. Liver passage of the IP-administered SaIONPs. SaIONPs-loaded circulating macrophages into the portal vein (black arrowheads) (a) and central vein (circle) (d). Cluster of SaIONPs-loaded macrophages (white arrows) on the liver capsule (b). Zonal accumulations of high SaIONPs-loaded hepatocytes (c). Homogeneous distribution of SaIONPs-loaded macrophages (black arrows) and focal distribution of SaIONPs-loaded hepatocytes (white arrowheads) in the liver lobule (e). Variation of the relative areas of SaIONPs deposits (RAD) in the liver of mice treated with 3 (D7), 7 (D14), and 10 (D21) doses of nanoparticles (Mann-Whitney U test, **p* < 0.05). Perls staining. Scale Bar=10µm.

The SaIONPs load of the liver estimated by the RAD index was 0,19±0,05 after 3 doses (day 7, cumulative dose of SaIONPs=105mg/kg body weight), 1,7±0,58 after 7 doses (day 14, cumulative dose of SaIONPs=244mg/kg body weight), and 1,99±0,43 after 10 doses (day 21, cumulative dose of SaIONPs=348mg/kg body weight).

In mice that received 14 doses (day 28, cumulative dose of SaIONPs=47mg/kg body weight), RAD was not measured due to the extent of liver necrosis lesions.

Data analysis showed that there were statistical differences only between mice that received 3 doses and mice that received 7 and 10 doses, respectively (**p*<0.05), suggesting that NP loading of the liver is limited (Figure 1f).

Histopathology

Liver histopathological changes associated with 3 doses of SaIONPs

From day 7 (3 doses of SaIONPs), subcapsular bands with histopathological changes were identified on the intelobar faces of the liver, where the SaIONPs aqueous dispersion probably persists longer (Figure 3 a,b).

Histopathological changes included the presence of giant hepatocytes with incompletely vacuolated clear cytoplasm and central nuclei, and were associated with hydropic degeneration.

Nuclei with condensed chromatin, karyolysis and also lytic necrosis of hepatocytes were observed (Figure 3 c,d).

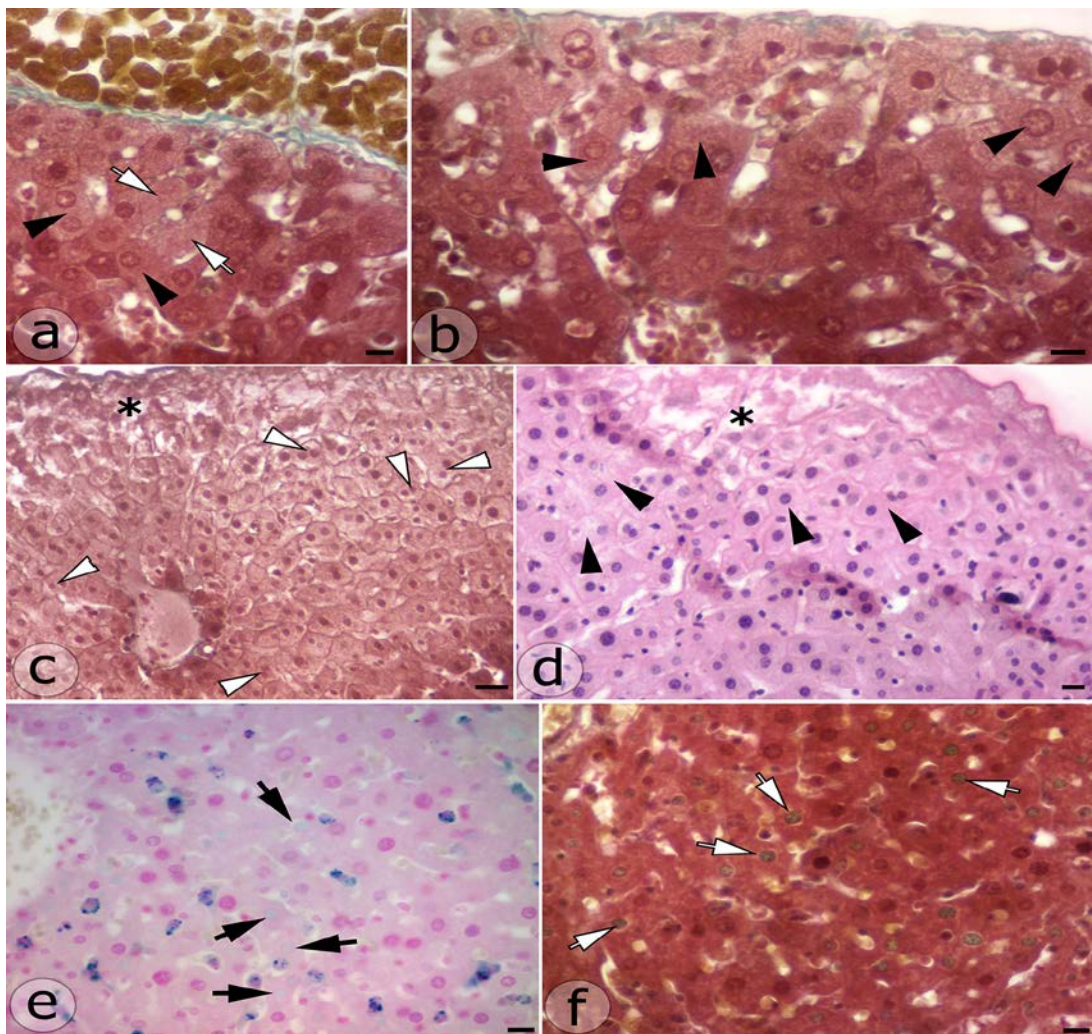


Figure 2. Subcapsular hydropic degeneration (black arrowheads) relative to (a) or distant from (b) extracapsular clusters of SaIONPs-loaded macrophages, associated with nuclear polymorphism, binucleate hepatocytes (white arrowheads), lytic necrosis of hepatocytes (white arrows) and foci of subcapsular liver necrosis (black star) (c, d). Karyolysis (black arrows) (e) associated with SaIONPs-loaded nuclei (white arrows) (f). Liver harvested on the 7th day of the experiment. Masson trichrome Goldner (a,b,c,f), Perls (e) and HE (d) stainings. Scale Bar=10µm

In areas with more advanced histopathological changes, liver necrosis was observed on the periphery of the area of hydropic degeneration (Figure 2 c,d).

This evolution of histopathological changes suggests that the lesion-inducing agent acted from outside the liver capsula. Perls staining ruled out the presence of deposits of SaIONPs in areas of hydropic degeneration.

Also, a feature of liver necrosis was the lack of inflammatory infiltrate.

Liver histopathological changes associated with 7 doses of SaIONPs

From day 14 of the experiment, high SaIONPs-loaded macrophages and hepatocytes were observed.

The SaIONPs-loaded macrophages were evenly dispersed, unlike the SaIONPs-loaded

hepatocytes, which have an irregular focal distribution (Figure 1e).

In addition to the nuclear polymorphism of SaIONPs-loaded hepatocytes, Perls staining showed intranuclear SaIONPs that was associated with nuclear changes: peripheral chromatin condensation, kariopycnosis, and karyolysis (Figure 2 e,f).

High SaIONPs-loading of the cytoplasm and nucleus observed in some hepatocytes (Figure 1e) was not associated with signs of cellular distress, suggesting the presence of additional aggression factors that modulate the toxic action of SaIONPs.

Foci of acidophilic pericentral necrosis with rich mononuclear inflammatory infiltrate were also observed (Figure 3 c,f).

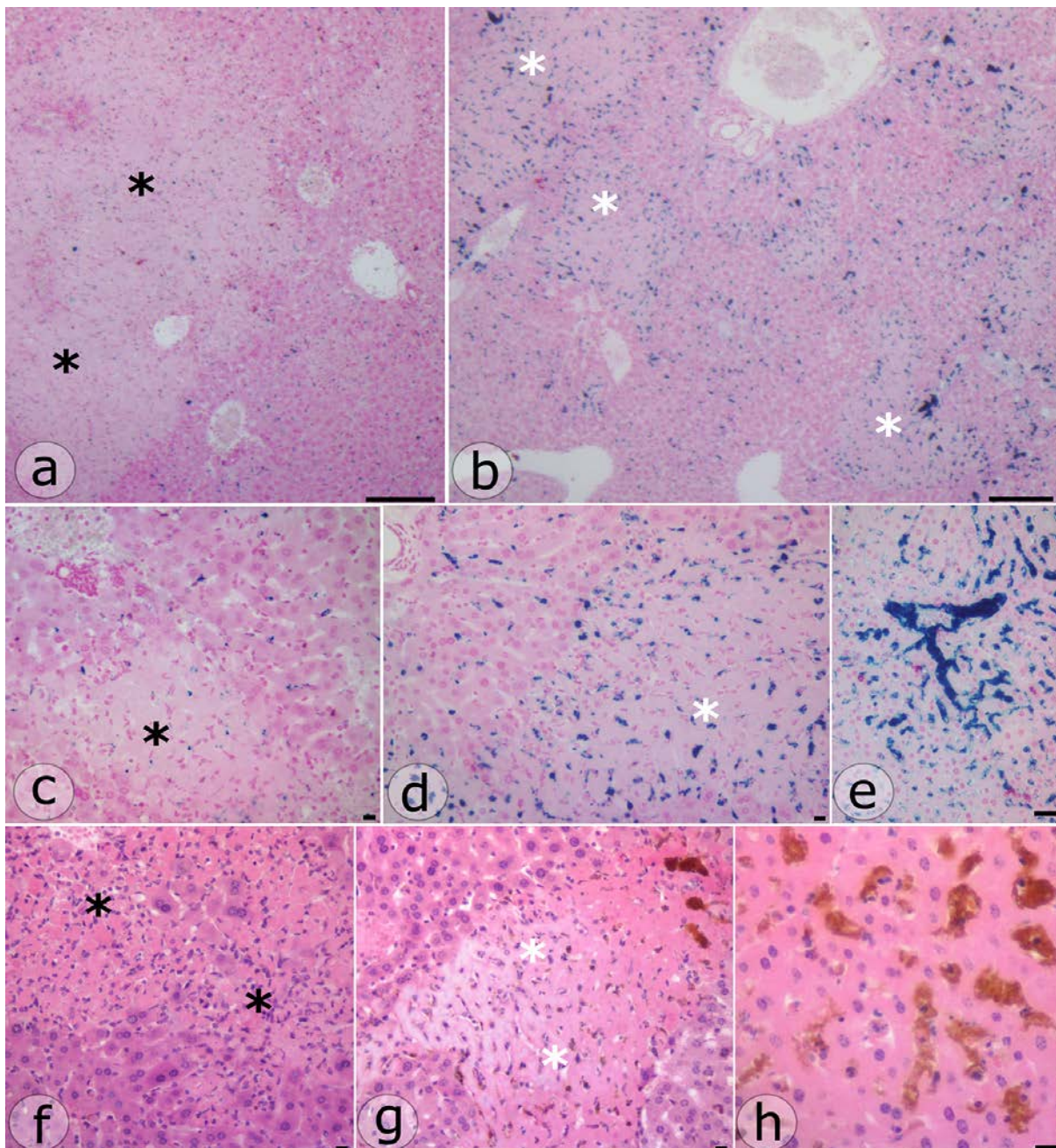


Figure 3. Extended (a, b) or centrilobular (c,d,f,g) liver necrosis, with massive accumulation of SaIONPs-loaded macrophages (b,d,g), which can block sinusoids and portal veins (h). Liver harvested on the 14th (c,f) or 21th (a,b,d,e,g h) day of the experiment. Perls (a-e) and HE (f-h) stainings. Scale Bar=20 μ m (a b), 10 μ m (c-h).

Liver histopathological changes associated with 10 doses of SaIONPs

On day 21 of the experiment, extensive areas of liver necrosis were identified (Figure 3a).

Some areas of necrosis showed massive accumulations of SaIONPs-loaded macrophages in the sinusoids (Figure 3b), which in some places led to their lumen blockage (Figure 3 e,h).

Liver histopathological changes associated with 14 doses of SaIONPs

SaIONPs accumulation in the necrosis foci due to hepatocytolysis was followed by massive SaIONPs loading of neighboring hepatocyte nuclei, which resulted in massive nucleolysis, while the appearance of hepatocyte cords remained (Figure 4).

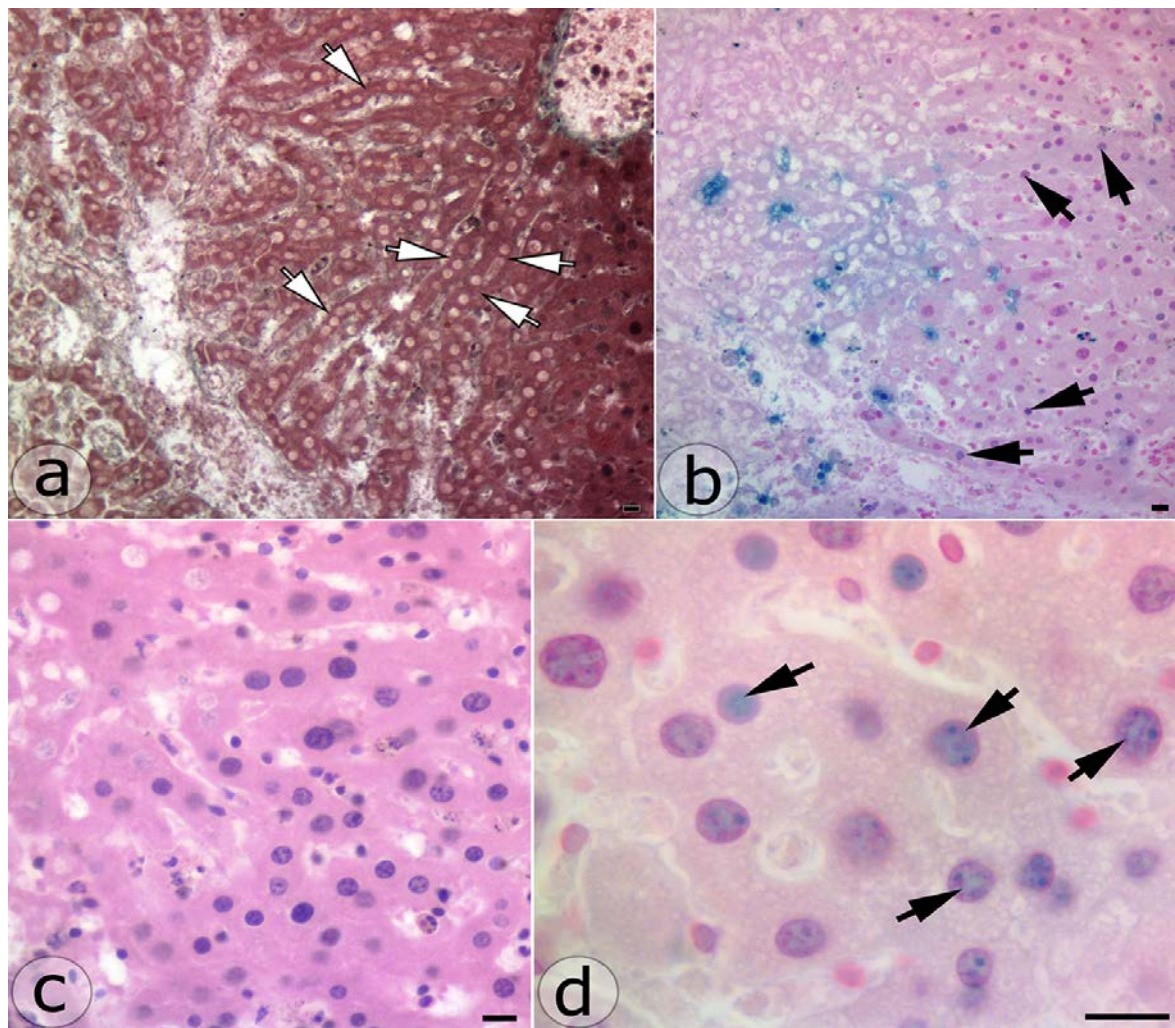


Figure 4. Extensive nucleolysis (white arrows) following the loading of perilesional hepatocytes nuclei (black arrows) with SaIONPs/Fe₃O₄ resulting from the degradation of SaIONPs-loaded cells in necrosis foci. Liver harvested on the 28th day of the experiment. Masson trichromic Goldner (a), Perls (b,d) and HE (c) stainings. Scale Bar=10µm.

Discussions

The toxicity of IONPs remains intensely debated, due to the multitude of studies conducted so far, some with contradictory results [2,16].

Some studies have shown that IONPs are biocompatible, without inducing toxicity affecting health [30].

Other studies have reported toxic effects of IONPs at the cellular level through multiple mechanisms [31].

Many factors that may influence the toxicity of IONPs have been described, some of them related to the conditions of the experiment (*in vivo* or *in vitro* testing, administration routes, cell types tested, model used), and others related to the physicochemical properties of the nanocomposites tested (nanoparticle size, presence or absence of the coating, types of

compounds used for the core coating, positive or negative surface charge) [16].

The stability of IONPs (characterized by dispersion zeta potential) is one of the main factors that define their biodistribution and toxicity, both *in vitro* and *in vivo* experiments [32].

The aqueous dispersion of SaIONPs used in this study had zeta potential=+50.5, which means that it has a high stability, which is mandatory for biomedical applications.

Pham et al. [32] showed that intraperitoneal administration of 90mg Fe/kg body weight IONPs, 10 and 25nm in diameter, did not induce histopathological changes in the rat liver.

The removal time of nanoparticles from the peritoneal cavity decreased with increasing nanoparticle diameter, and for those of 10nm it was 48h.

The increase in the level of anti-F4/80 cells in the liver, spleen and large omentum has demonstrated their role in the uptake of intraperitoneal nanoparticles.

The results of our study showed that histopathological changes in the liver were identified starting with the cumulative dose of 62mg/kg body weight of Fe₃O₄, and had a peripheral, subcapsular distribution, suggesting an extracapsular induction factor.

The clusters of high SaIONPs-loaded macrophage, which we have identified on the surface of the liver, but also of other abdominal viscera, can lead to the release of salicylic acid by degradation of intracytoplasmic-loaded SaIONPs.

The release of salicylic acid into the peritoneal cavity may explain the onset of subcapsular liver damage, which has been observed since mice sacrificed on day 7.

SaIONPs reach the liver through the portal vein, both in the form of agglomerations visible in light microscopy and especially loaded in circulating macrophages.

Aggregates of SaIONPs are responsible for the subsequent loading of hepatocytes.

Because SaIONPs have been identified by Prussian blue staining, it is not known whether intracytoplasmic deposits in the loaded hepatocytes or macrophages contain SaIONPs or only Fe₃O₄.

So far, we have not identified reliable methods to allow this difference in liver samples.

Macropinocytosis is the main route of IONPs internalization in macrophages [33].

Wang et al. [34] showed that the IONPs internalization in macrophages can also be achieved caveolae-mediated endocytosis, and the internalization of nanoparticles of 20-40nm was 5-10 times higher than those of 100nm.

Internalization by a caveolae-mediated endocytosis allowed IONPs transport into the nucleus [35], and explained tendency of smaller nanoparticles to accumulate intranuclear.

SaIONPs used by us had an average hydrodynamic diameter of 73nm, but the aqueous dispersion also contains nanoparticles with a smaller diameter, because the nanosynthesis process does not allow accurate control of the diameter and complete removal of small nanoparticles.

In long-term administration, these small SaIONPs can accumulate intranuclear by caveolae-mediated endocytosis and thus explain

the intranuclear loading of SaIONPs observed by us.

Studying the intracellular trafficking of IONPs of different sizes functionalized with polystyrene, Sandin et al. [36] showed that nanoparticles passed into endosomes to eventually reach the lysosomes, and the rate of transfer decreases with increasing diameter of the nanoparticles.

Also, a small part of the nanoparticles have been identified in the recycling endosomes, and can be redirected back to the cell membrane.

In another study, Behzadi et al. [37] have shown that some macrophage-loaded IONPs can escape from endosomes before they fuse with lysosomes, thus avoiding lysosomal degradation.

The high enzymatic content and acidic environment of lysosomes [38] are factors that can cause the degradation of nanoparticles.

These findings, as well as a series of observations on the evolution of liver damage presented in this study allow us to state that the cytoplasm of liver macrophages and hepatocytes may contain either SaIONPs in endosomes or escaped from endosomes, or Fe₃O₄ resulting from the removal of SaIONPs salicylic acid in lysosomes.

First, we identified high intracytoplasmic and intranuclear SaIONPs-loaded hepatocytes that showed no microscopic signs of cellular distress.

In other areas, with large accumulations of loaded macrophages, we observed hepatocytes with nuclear changes up to karyolysis, showing fine traces of intranuclear and intracytoplasmic SaIONPs.

These observations suggest that lesions of hepatocytes in areas rich in loaded macrophages may be attributed to salicylic acid released as a result of SaIONPs lysosomal degradation.

The incrimination of salicylic acid as a factor in the induction of histopathological changes in the liver is supported by the features of liver damage, similar to salicylate intoxication, (hydropic degeneration, reduced inflammatory infiltration and localized necrosis [39]).

At a dose of 244mg/kg body weight SaIONPs (145mg/kg body weight Fe₃O₄) we observed liver necrosis lesions, which have been reported by other authors, but at a dose of 300mg/kg body weight of Fe₃O₄ [19].

Our results show that the toxicity of Fe₃O₄ was potentiated by the toxicity of the salicylic acid coating, possibly by increasing the permeability of the membranes, a specific effect of salicylates [25].

Conclusions

The increased stability of the nanoparticles conferred by the salicylic acid coating was accompanied by increased toxicity.

The cumulative dose of 105mg/kg body weight SaIONPs (6mg/kg body weight of Fe₃O₄) induced histopathological changes in the subcapsular region of the mouse liver, possible by the release of salicylic acid into the peritoneal cavity.

The cumulative dose of 244mg/kg body weight SaIONPs (145mg/kg body weight of Fe₃O₄) induced centrolobular necrosis, which requires the use of lower doses in biological applications.

However, this may prove to be beneficial in the case of targeted accumulation of SaIONPs.

Conflict of interests

None to declare.

References

- Ajinkya N, Yu X, Kaithal P, Luo H, Somani P, Ramakrishna S. Magnetic Iron Oxide Nanoparticle (IONP) Synthesis to Applications: Present and Future. *Materials (Basel)*, 2020, 13(20):4644.
- Arias LS, Pessan JP, Vieira APM, Lima TMT, Delbem ACB, Monteiro DR. Iron Oxide Nanoparticles for Biomedical Applications: A Perspective on Synthesis, Drugs, Antimicrobial Activity, and Toxicity. *Antibiotics (Basel)*, 2018, 7(2):46.
- Quinto CA, Mohindra P, Tong S, Bao G. Multifunctional superparamagnetic iron oxide nanoparticles for combined chemotherapy and hyperthermia cancer treatment. *Nanoscale*, 2015, 7(29):12728-12736.
- Panagiotopoulos N, Duschka RL, Ahlborg M, Bringout G, Debbeler C, Graeser M, Kaethner C, Lütke-Buzug K, Medimagh H, Stelzner J, Buzug TM, Barkhausen J, Vogt FM, Haegele J. Magnetic particle imaging: Current developments and future directions. *Int J Nanomedicine*, 2015, 10:3097-3114.
- Dadfar SM, Roemhild K, Drude NI, von Stillfried S, Knüchel R, Kiessling F, Lammers T. Iron oxide nanoparticles: Diagnostic, therapeutic and theragnostic applications. *Adv Drug Deliv Rev*, 2019, 138:302-325.
- Predoi MC, Mîndrilă I, Buteică SA, Purcaru ȘO, Mihaiescu DE, Mărginean OM. Iron Oxide/Salicylic Acid Nanoparticles as Potential Therapy for B16F10 Melanoma Transplanted on the Chick Chorioallantoic Membrane. *Processes*, 2020, 8:706.
- Mîndrilă B, Buteică SA, Mîndrilă I, Mihaiescu DE, Mănescu MD, Rogoveanu I. Administration Routes as Modulators of the Intrahepatic Distribution and Anti-Anemic Activity of Salicylic Acid/Fe₃O₄ Nanoparticles. *Biomedicines*, 2022, 23, 10(5):1213.
- Friedrich RP, Cicha I, Alexiou C. Iron Oxide Nanoparticles in Regenerative Medicine and Tissue Engineering. *Nanomaterials (Basel)*, 2021, 11(9):2337.
- Prabhu S, Mutalik S, Rai S, Udupa N, Rao BSS. PEGylation of superparamagnetic iron oxide nanoparticle for drug delivery applications with decreased toxicity: an in vivo study. *J Nanopart Res*, 2015, 17:412.
- Makadia HK, Siegel SJ. Poly lactic-co-glycolic acid (PLGA) as biodegradable controlled drug delivery carrier. *Polymers (Basel)*, 2011, 3(3): 1377-1397.
- Soares PI, Machado D, Laia C, Pereira LC, Coutinho JT, Ferreira IM, Novo CM, Borges JP. Thermal and magnetic properties of chitosan-iron oxide nanoparticles. *Carbohydr Polym*, 2016, 149: 382-390.
- Soares PI, Lochte F, Echeverria C, Pereira LC, Coutinho JT, Ferreira IM, Novo CM, Borges JP. Thermal and magnetic properties of iron oxide colloids: Influence of surfactants. *Nanotechnology*, 2015, 26(42):425704.
- Buteică SA, Mihaiescu DE, Rogoveanu I, Mărgăritescu DN, Mîndrilă I. Chick chorioallantoic membrane model as a preclinical tool for nanoparticles biology study. *Rom Biotechnol Lett*, 2016, 21(4):11688-11694.
- Mu Q, Kievit FM, Kant RJ, Lin G, Jeon M, Zhang M. Anti-HER2/neu peptide-conjugated iron oxide nanoparticles for targeted delivery of paclitaxel to breast cancer cells. *Nanoscale*, 2015,7(43): 18010-18014.
- Feng Q, Liu Y, Huang J, Chen K, Huang J, Xiao K. Uptake, distribution, clearance, and toxicity of iron oxide nanoparticles with different sizes and coatings. *Sci Rep*, 2018, 8(1):2082.
- Wei H, Hu Y, Wang J, Gao X, Qian X, Tang M. Superparamagnetic iron oxide nanoparticles: cytotoxicity, metabolism, and cellular behavior in biomedicine applications. *Int J Nanomedicine*, 2021,16: 6097-6113.
- Yang L, Kuang H, Zhang W, Aguilar ZP, Xiong Y, Lai W, Xu H, Wei H. Size dependent biodistribution and toxicokinetics of iron oxide magnetic nanoparticles in mice. *Nanoscale*, 2015, 7(2): 625-636.
- Gokduman K, Bestepe F, Li L, Yarmush ML, Usta OB. Dose-, treatment- and time-dependent toxicity of superparamagnetic iron oxide nanoparticles on primary rat hepatocytes. *Nanomedicine (Lond)*, 2018, 13(11):1267-1284.
- Parivar K, Malekvand Fard F, Bayat M, Alavian SM, Motavaf M. Evaluation of iron oxide nanoparticles toxicity on liver cells of BALB/c rats. *Iran Red Crescent Med J*, 2016, 18(1):e28939.
- Valdiglesias V, Fernández-Bertólez N, Kiliç G, Costa C, Costa S, Fraga S, Bessa MJ, Pásaro E, Teixeira JP, Laffon B. Are iron oxide nanoparticles safe? Current knowledge and future perspectives. *J Trace Elem Med Biol*, 2016, 38:53-63.
- Ansari MO, Parveen N, Ahmad MF, Wani AL, Afrin S, Rahman Y, Jameel S, Khan YA, Siddique HR, Tabish M, Shadab GGHA. Evaluation of DNA interaction, genotoxicity and oxidative stress induced by iron oxide nanoparticles both in vitro and in vivo: attenuation by thymoquinone. *Sci Rep*, 2019, 9(1): 6912.

22. Levada K, Pshenichnikov S, Omelyanchik A, Rodionova V, Nikitin A, Savchenko A, Schetin I, Zhukov D, Abakumov M, Majouga A, Lunova M, Jirsa M, Smolková B, Uzhytchak M, Dejneka A, Lunov O. Progressive lysosomal membrane permeabilization induced by iron oxide nanoparticles drives hepatic cell autophagy and apoptosis. *Nano Converg*, 2020, 7(1):17.
23. Gaharwar US, Kumar S, Rajamani P. Iron oxide nanoparticle-induced hematopoietic and immunological response in rats. *RSC Adv*, 2020, 10(59):35753-35764.
24. Xiao K, Li Y, Luo J, Lee JS, Xiao W, Gonik AM, Agarwal RG, Lam KS. The effect of surface charge on in vivo biodistribution of PEG-oligocholic acid based micellar nanoparticles. *Biomaterials*, 2011, 32(13):3435-3446.
25. Kajii H, Horie T, Hayashi M, Awazu S. Effects of salicylic acid on the permeability of the plasma membrane of the small intestine of the rat: a fluorescence spectroscopic approach to elucidate the mechanism of promoted drug absorption. *J Pharm Sci*, 1986, 75(5):475-478.
26. Mihaiescu DE, Buteică A., Neamțu J, Istrati D, Mîndrilă I. Fe₃O₄/Salicylic acid nanoparticles behavior on chick CAM vasculature. *J Nanopart Res*, 2013, 15:1-10.
27. Jahn MR, Nawroth T, Fütterer S, Wolfrum U, Kolb U, Langguth P. Iron oxide/hydroxide nanoparticles with negatively charged shells show increased uptake in Caco-2 cells. *Mol Pharm*, 2012, 9(6): 1628-1637.
28. Mîndrilă I, Osman A, Mîndrilă B, Predoi, MC, Mihaiescu DE, Buteică SA. Phenotypic switching of B16F10 melanoma cells as a stress adaptation response to Fe₃O₄/Salicylic Acid nanoparticle therapy. *Pharmaceuticals (Basel)*, 2021,14(10): 1007.
29. Grattagliano I, Bonfrate L, Diogo CV, Wang HH, Wang DQ, Portincasa P. Biochemical mechanisms in drug-induced liver injury: certain ties and doubts. *World J Gastroenterol*, 2009, 15(39):4865-4876.
30. Paik SY, Kim JS, Shin SJ, Ko S. Characterization, quantification, and determination of the toxicity of iron oxide nanoparticles to the bone marrow cells. *Int J Mol Sci*, 2015,16(9):22243-22257.
31. He C, Jiang S, Jin H, Chen S, Lin G, Yao H, Wang X, Mi P, Ji Z, Lin Y, Lin Z, Liu G. Mitochondrial electron transport chain identified as a novel molecular target of SPIO nanoparticles mediated cancer-specific cytotoxicity. *Biomaterials*, 2016, 83:102-114.
32. Pham BTT, Colvin EK, Pham NTH, Kim BJ, Fuller ES, Moon EA, Barbey R, Yuen S, Rickman BH, Bryce NS, Bickley S, Tanudji M, Jones SK, Howell VM, Hawckett BS. Biodistribution and clearance of stable superparamagnetic maghemite iron oxide nanoparticles in mice following intraperitoneal administration. *Int J Mol Sci*, 2018, 19(1):205.
33. Wu M, Guo H, Liu L, Liu Y, Xie L. Size-dependent cellular uptake and localization profiles of silver nanoparticles. *Int J Nanomedicine*, 2019, 14: 4247-4259.
34. Wang Z, Tiruppathi C, Minshall RD, Malik AB. Size and dynamics of caveolae studied using nanoparticles in living endothelial cells. *ACS Nano*, 2009, 3(12):4110-4116.
35. Gamboa JM, Leong KW. In vitro and in vivo models for the study of oral delivery of nanoparticles. *Adv Drug Deliv Rev*, 2013, 65(6):800-810.
36. Sandin P, Fitzpatrick LW, Simpson JC, Dawson KA. High-speed imaging of Rab family small GTPases reveals rare events in nanoparticle trafficking in living cells. *ACS Nano*, 2012, 6(2): 1513-1521.
37. Behzadi S, Serpooshan V, Tao W, Hamaly MA, Alkawareek MY, Dreaden EC, Brown D, Alkilany AM, Farokhzad OC, Mahmoudi M. Cellular uptake of nanoparticles: journey inside the cell. *Chem Soc Rev*, 2017, 46(14):4218-4244.
38. Trapp S, Rosania GR, Horobin RW, Kornhuber J. Quantitative modeling of selective lysosomal targeting for drug design. *Eur Biophys J*, 2008, 37(8):1317-1328.
39. Starko KM, Mullick FG. Hepatic and cerebral pathology findings in children with fatal salicylate intoxication: further evidence for a causal relation between salicylate and Reye's syndrome. *Lancet*, 1983, 1(8320):326-329.

**Corresponding Author: Sandra-Alice Buteică, Faculty of Pharmacy,
University of Medicine and Pharmacy of Craiova, 200349 Craiova, Romania
e-mail: alice.buteica@umfcv.ro**